Materials and Design 30 (2009) 109–114

Contents lists available at ScienceDirect

Materials and Design

journal homepage: www.elsevier.com/locate/matdes

Fiber laser-GMA hybrid welding of commercially pure titanium

Cui Li [a,*], Kutusna Muneharua [a], Simizu Takao [b], Horio Kouji [b]

[a] Graduate School of Engineering, Nagoya University, Nagoya 464 8603, Japan
[b] Daido Steel Co., Ltd., 2-30 Daido-cho, Minami-ku, Nagoya 457-8545, Japan

ARTICLE INFO

Article history:
Received 28 November 2007
Accepted 16 April 2008
Available online 28 April 2008

Keywords:
A. non-ferrous metals and alloys
D. welding
E. mechanical

ABSTRACT

Fiber laser-gas metal arc (GMA) hybrid welding process was introduced to weld of commercially pure titanium (CP-Ti) of 1.5 mm in thickness. Effect of welding parameters on the hybrid weldability was investigated concerning the bead shape, hardness, tensile properties and microstructures of welded joints compared with those of a fiber laser welded joint. As a result, fiber laser-GMA hybrid welding process has been shown to weld of CP-Ti sheets in 1.5mm thickness at speeds of up to 9 m/min. In addition, fiber laser-GMA hybrid welding produces higher Vickers hardness and tensile strength than that of the base metal. Compared with the laser welded joints, it is obvious that the hybrid welded joints have better combination of strength and ductility.

1. Introduction

The high specific weight, excellent corrosion resistance, high temperature performance and biocompatibility of titanium make it attractive to many industries, such as aerospace, defense, petrol-chemical, nuclear energy and medical industry [1].

With the increased use of CP-Ti, the joining of titanium has become more and more important [2]. Most research on welding of CP-Ti has utilized gas tungsten arc welding (GTAW) in an inert gas atmosphere [3–6]. However, GTAW in thinner materials is done at much slower speeds and therefore low deposition rates. Because of the higher heat input the welded parts are more likely to be distorted [7]. Gas metal arc welding (GMAW) may increase efficiency and decrease welding cost but cannot produce high quality welds at higher travel speeds. The drawbacks of GMAW process are related to the instability of the arc [1] and excessive spatter [8]. Other researches are concerned with friction stir welding (FSW) [2] and electron beam welding (EBW) [3] of CP-Ti. However, the problems with EBW involve the use of high vacuum and difficulties in seam-tracking exactly the required joint line [9]. FSW of titanium has not yet been demonstrated as a viable production process, primarily due to excessive tool wear and lack of joint performance data [9]. Thus, new methods of welding are continuously being developed to overcome these limitations.

There is an increasing interest on the laser welding of titanium alloys to expand their fields of application with utilizing CO_2-laser [3] and Nd:YAG laser [7,10]. As a non-contact process, a major advantage of laser welding is low welding stresses and consequent low risk of distortion. This is achieved by the high energy density of the laser beam producing a small pool and by the high travel speed. However, disadvantages of the wider use of the laser welding process are the insufficient gap bridging ability and the required precision in positioning [11]. Furthermore, the wall plug efficiency of CO_2 and Nd:YAG lasers is low [12]. The combination of laser welding with either GTAW or GMAW is referred to as hybrid welding [1]. The hybrid laser welding process has proven to resolve these drawbacks of laser welding, while maintaining the key advantages of laser welding and even improving the welding speed and penetration [13]. High power fiber lasers are a new developed laser, which has attracted a great deal of attentions in the industrial fields, due to its multiple advantages [14]. The fiber lasers are very compact, robust and excel in terms of performance, power scalability, reliability, efficiency and operating lifetimes. The lasers are highly efficient with more than 20% wall plug efficiency, reducing electrical requirements and also provide better beam quality than the conventional solid-stage lasers [15]. Since kilowatt level fiber lasers have been in use for only a couple of years, there is very little published information on laser hybrid welding with fiber laser.

In this study, fiber lasers-GMA hybrid welding process was investigated for welding of CP-Ti, particularly with regard to weld quality. Additional benefits, primarily related to gap bridging capability and productivity, may be realized by using this new fiber laser-GMA hybrid welding process. The primary objective of the work was to compare the performance of the fiber laser-GMA hybrid welding with fiber laser welding process in joining of CP-Ti. The emphasis was placed on an evaluation of the weld bead shape, hardness, microstructure and tensile properties of the fiber laser-GMA hybrid welded joints.

* Corresponding author.
E-mail address: cuilikr@yahoo.com (C. Li).

0261-3069/$ - see front matter © 2008 Elsevier Ltd. All rights reserved.
doi:10.1016/j.matdes.2008.04.043

2. Experimental method

2.1. Materials

CP-Ti grade 2 titanium (JIS H 4600 TP 340C) in the dimension of 200 × 50 × 1.5 mm was used in the study. The specimen surfaces were chemically cleaned by acetone before welding to eliminate surface contamination. Filler metal in the form of spooled wire was developed by Daido Steel Co., Ltd. equivalent to AWS ERTi-2 with 1.2 mm in diameter. The chemical compositions of the base metal and the filler wires are shown in Table 1.

2.2. Welding equipments and conditions

Full penetration I-butt joints were made using a 2kW YLR-2000 Yb fiber laser in combination with a Digital Auto DM350 GMAW power supply. The fiber lasers with an emission wave length of 1.07 μm can deliver in continuous wave (CW) mode through an output fiber core diameter of 100 μm. The focusing head is 6° tilted to avoid back reflection and potential damage to the fiber termination module. The laser welding system had a 200 mm collimatation lens and a 200 mm focusing lens. The beam parameter product (BPP) of the laser beam at the focal point was 4.2 mm mrad. The focus position during the experiments was kept on the top surface of specimens. The fiber laser system and the GMAW torch were fixed to a 6-axial welding robot and the torch at 45° from vertical as shown in Fig. 1.

Throughout the experiments, the welding operation was carried out in an argon-filled plastic bag to completely exclude of contaminating gases from the weld. The primary, trailing and back shielding gas supplied by ultra high purity argon gas were at flow rates of 20 L/min, 15 L/min and 15 L/min. During welding, a range of laser powers (from 1 kW to 2 kW) and travel speeds (from 4 m/min to 9 m/min) were selected first, and the voltage and currents were varied from 22 to 30 V and from 200 to 300 A to form a reliable keyhole and stable the arc correspondingly.

2.3. Testing conditions

After welding, the specimens were cut transversely of the welds and prepared for metallographic inspection by mounting, mechanical polishing and etching in a Kroll reagent to display bead shape and microstructure. Microstructure characterization was performed using a laser scanning microscope. The metallurgical phases of the base metal and weld joints were identified by a magnifier X-ray diffraction (XRD) analysis with Cu Kα radiation. Vickers microhardness indentations of the welded joints were placed across the weld using a Vickers hardness tester with 100 g load. The oxygen intensity percent obtained in the welded joints and base metal using a scanning electron microscope (SEM) coupled with energy dispersive X-ray (EDX) analysis. The tensile tests of the prepared specimens were carried out on a uniaxial tensile tester on the welded joints obtained at welding speeds of from 4 m/min to 9 m/min at a laser power of 2 kW, with strain rates of 1 mm/min at room temperature.

3. Results and discussion

3.1. Weld bead

The bead appearance and cross section of laser-GMA hybrid welded joint at a speed of 9 m/min compared with that of fiber laser welded joints is shown in Fig. 2. Full penetration welds with regular weld shapes are obtained at a travel speed of 9 m/min by using these two welding processes. One of the most important observations is that the welds surfaces showed bright silver color, smooth and little deformation, which indicates the good shielding of the molten pool [14]. The butt joints welded by fiber laser welding have a narrow and near parallel weld shape, and the narrow heat affected zone (HAZ) collectively produce very little workpiece distortion. However, there is a slightly undercut in weld bead of laser welds. In the case of fiber laser-GMA hybrid welding process, the welded joint of CP-Ti have a slightly protruding top surface with significantly wider HAZ. Thus, full penetrations welds without undercut have been obtained by the hybrid welding process with the same high travel speeds as in laser welding process, but the width of HAZ is increased.

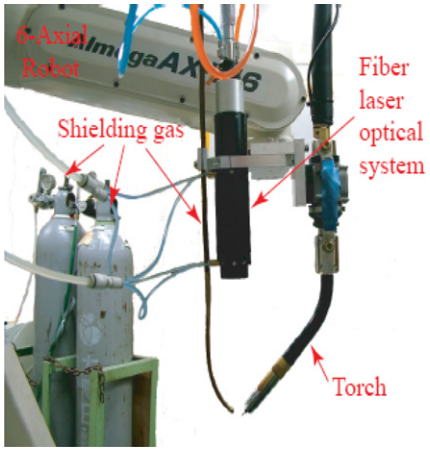

Fig. 1. Fiber laser-GMAW hybrid welding system.

3.2. Microhardness of the welds

Fig. 3 shows Vickers hardness indentations placed across the two welds (from the weld centerline through the HAZ and into the base metal). The hardness of base metal is about 150 Hv, whereas the weld metal is slightly higher than this figure varied with between 160 and 220 HV. Hardness of the HAZ is about similar to that of base metal, indicating that the HAZ does not have much to do with the overall hardness. As it gets closer to the center of the weld metal from the HAZ, the hardness abruptly increases, and the peak hardness of laser weld and hybrid weld reaches 190 and 212 HV, respectively. The hardness of hybrid welded joints is higher, and the hardness distribution at the center is wider than that of the laser welded joints, whereas the laser welded joints show narrower distribution and lower hardness. Both laser welds and laser-GMA hybrid welds which are produced in CP-Ti are harder than the base metal. This illustrates the high weld hardness produced when laser welding and laser-GMA hybrid welding of a pure titanium. According to a literature [6], the increase in hardness is directly related to the oxygen concentration in the weld. The result of oxygen intensity percent obtained in the two welded joints using a SEM coupled with EDX analysis is shown in Fig. 4. Due to the nature of EDX analysis, these values can only be used for comparative purposes, and are not actual values. It is seen that the oxygen intensity percent of fusion zone is a little higher than the base metal in both laser-GMA hybrid and laser welded joints. However, the oxygen content in titanium, although the major element concerned, does not alone determine the weld hardness for a given cooling rate. The final hardness result depends on the interaction of cooling rate with the composition including oxygen and nitrogen contents [16]. Thus, it is immediately evident from these results that the interaction of cooling rate with the composition including oxygen and nitrogen contents on the microhardness of the welded joints is significant.

Table 1
Chemical composition and mechanical properties of the base metal and filler wires

Materials	Chemical composition (wt%)						Mechanical properties			
	N	C	H	Fe	O	Ti	Y.S. (MPa)	T.S. (MPa)	Elongation (%)	Hardness (HV)
CP-Ti	0.03	0.10	0.015	0.30	0.25	Balance	215	340	23	150
Filler wire	0.02	0.02	0.008	0.30	0.25	Balance	–	380	–	–

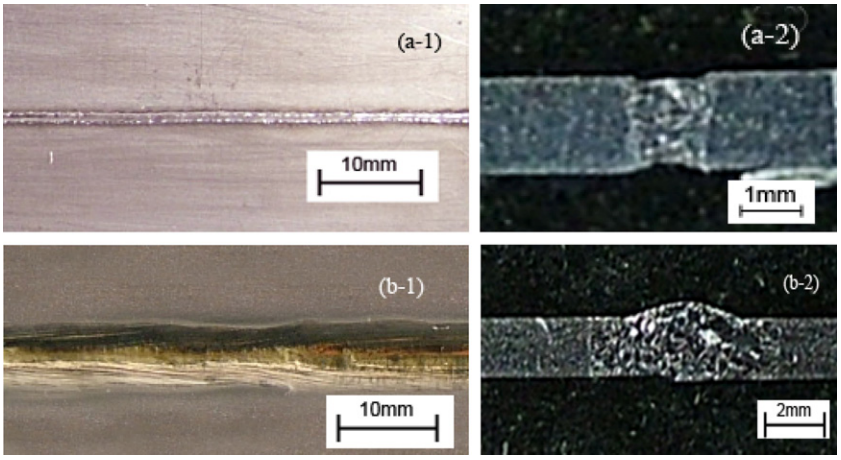

Fig. 2. Comparison of welded joints at a welding speed of 9 m/min: (a-1) top bead appearance of a fiber laser welded joint; (a-2) cross section of a fiber laser welded joint; (b-1) Top bead appearance of a laser-GMA hybrid welded joint; (b-2) cross section of a laser-GMA hybrid welded joint.

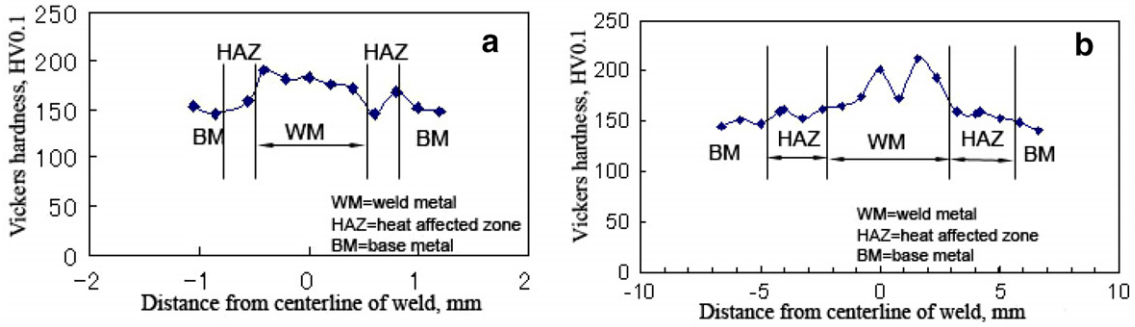

Fig. 3. Hardness plot taken across the welded joint, laser power P = 2 kW, welding speed v = 9 m/min: (a) fiber laser welding; (b) hybrid welding, defocusing distance = 0 mm, arc-laser distance = 1 mm, arc voltage = 20 V, welding current = 220 A.

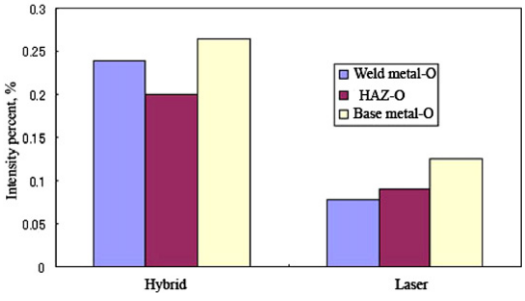

Fig. 4. Oxygen profile comparison in the welded joints.

3.3. Tensile properties

Fig. 5 shows that the tensile strength and elongation of two welded joints in comparison with that of base metal. For the laser-GMA hybrid welded joints, fracture occurs at the base metal; but in the case of the laser welded joints, fracture occurs at the weld metal. It is clear that the tensile strength of base metal is largely achieved in the two welded joints, while a slight ductility loss occurs due primarily to the coarser microstructure that forms in the fusion zone. However, the hybrid welded joints have higher elongation than those of the fiber laser welded joints. Thus, hybrid welded joints have higher tensile strengths and better elongation than those of the fiber laser welded joints. Compared with the laser welded joints, it is obvious that the hybrid welded joints have better combination of strength and ductility. As in all materials, the mechanical properties of the weldments are strongly related to their microstructures and chemical composition [4].

3.4. Microstructure of welding joints

Titanium undergoes an allotropic phase transformation at 882 °C (alpha (HCP) ⇌ beta (BCC)) [13]. During welding, the material in the fusion zone has been heated to 882 °C or higher, resulting in transformation to β phase. As the weld cools through the β transus, the cooling rate from the β phase field has a controlling influence on the resulting microstructure in a CP-Ti [17]. Consequently, depending on processing parameters, the microstructure of titanium can vary widely. Therefore, XRD analysis of the base metal and welded joints were carried out to determine which phases (either α-Ti or β-Ti) were present by observing their respective diffraction patterns. The phases measurements performed using Cu Kα radiation at 40 kV and 20 mA in the 2θ window from 20 to 80°, are shown in Fig. 6. The main diffraction peaks of base metal reveals the presence of the α-Ti hcp phase. Alpha phases are identified for the HAZ and weld metal in two welded joints, compared with the diffraction pattern shown in the base metal.

The microstructure of the fiber laser welded joints at a laser power of 2 kW is shown in Fig. 7. The welding thermal cycle in fiber laser welding changes the microstructure of base metal from equiaxed alpha to a mixed coarse alpha. The significant grain coarsening has occurred in the HAZ immediately adjacent to the base metal and the degree of grain coarsening increases as the grains move towards the centre of the fusion zone. Fig. 7a shows only coarse columnar alpha appears in the fiber laser weld metal

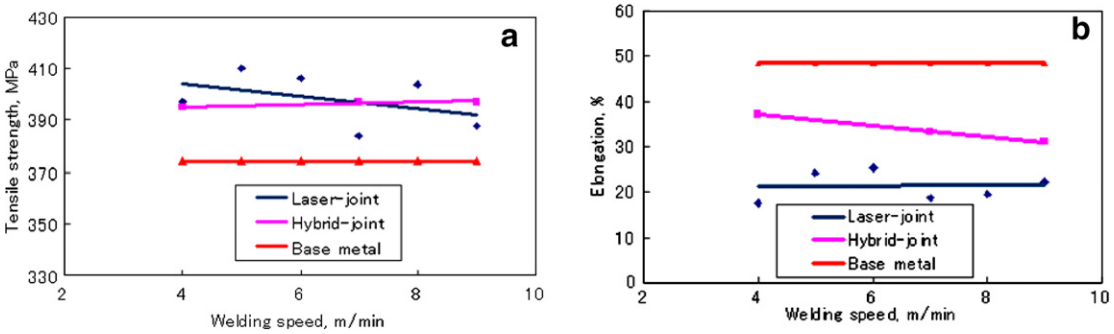

Fig. 5. Comparison of tensile properties of welded joint with base metal: (a) tensile strength; (b) elongation.

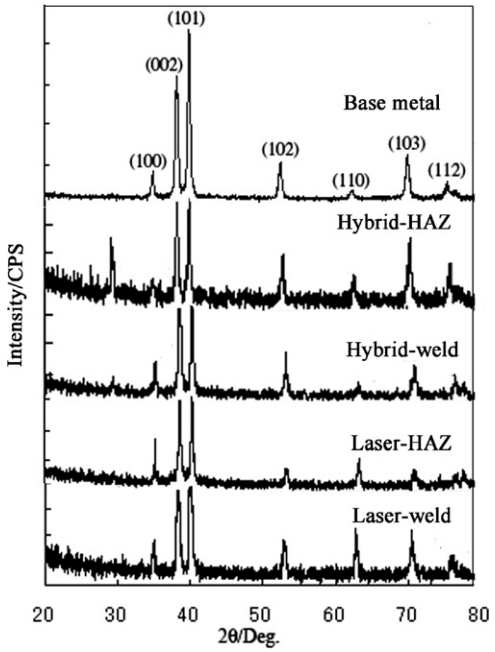

Fig. 6. Calculated diffraction pattern in welded joints and base metal.

when welding speed is 4 m/min. In the case of welding speeds of above 5 m/min as shown in Fig. 7b–d that the microstructures at the weld centerline appears a smaller amount of fine-grained acicular alpha. With increasing welding speeds, fine-grained acicular alpha occurs in the weld centerline, i.e., higher welding speeds resulted in the formation of acicular alpha phase transformed from the β phase. Because the higher welding speed leads to higher cooling rate, it can be said that high cooling rate resulted in the formation of finer acicular alpha phase. With these observations, it can be found that the welding speed and cooling rate are critical parameters in controlling the microstructure of the fiber laser welded joints.

Fig. 8 is an optical micrograph of the laser-GMA hybrid welds. It is obvious that the difference in microstructure occurs at the fusion zone of laser-GMA hybrid welded joints compared with those in laser welded joints. Fig. 8b is higher magnification micrographs of the regions in the HAZ immediately adjacent to the base metal. The microstructure is the serrated alpha (pointed by arrow S) characterized by irregular grain size and jagged grain boundaries. Fig. 8c shows the appearance of the fusion boundary near to weld metal, and the microstructures comprise serrated alpha and fine-grained acicular alpha (pointed by arrow A). Fig. 8d and e shows the details of the weld metal microstructure, dominated by acicular alpha, coarse serrated alpha and twins (pointed by arrow T). The appearance of the twins is the distinct microstructure feature in the weld metal. These twins with different size and random

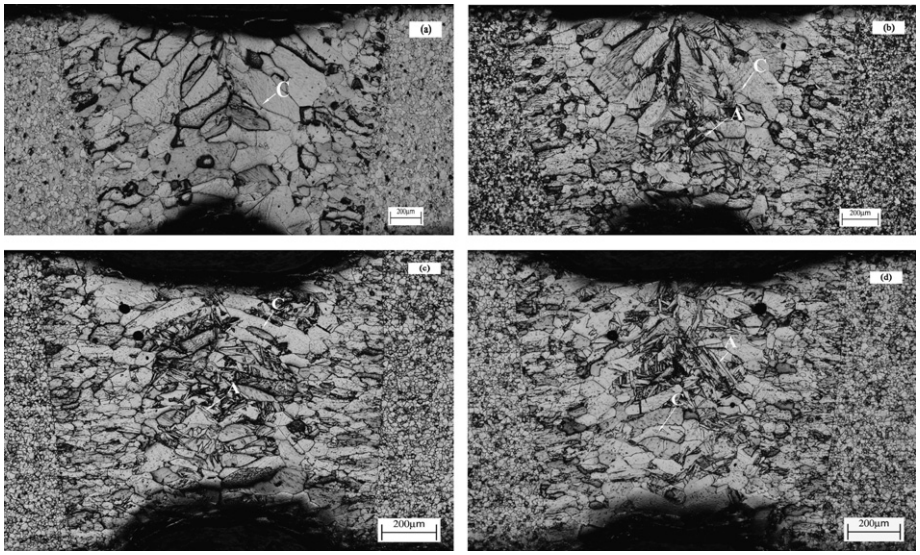

Fig. 7. Microstructure of fiber laser welded joints at a laser power of 2 kW: welding speeds (a) v = 4 m/min; (b) v = 5 m/min; (c) v = 7 m/min; (d) v = 8 m/min. Etchant: Kroll reagent.

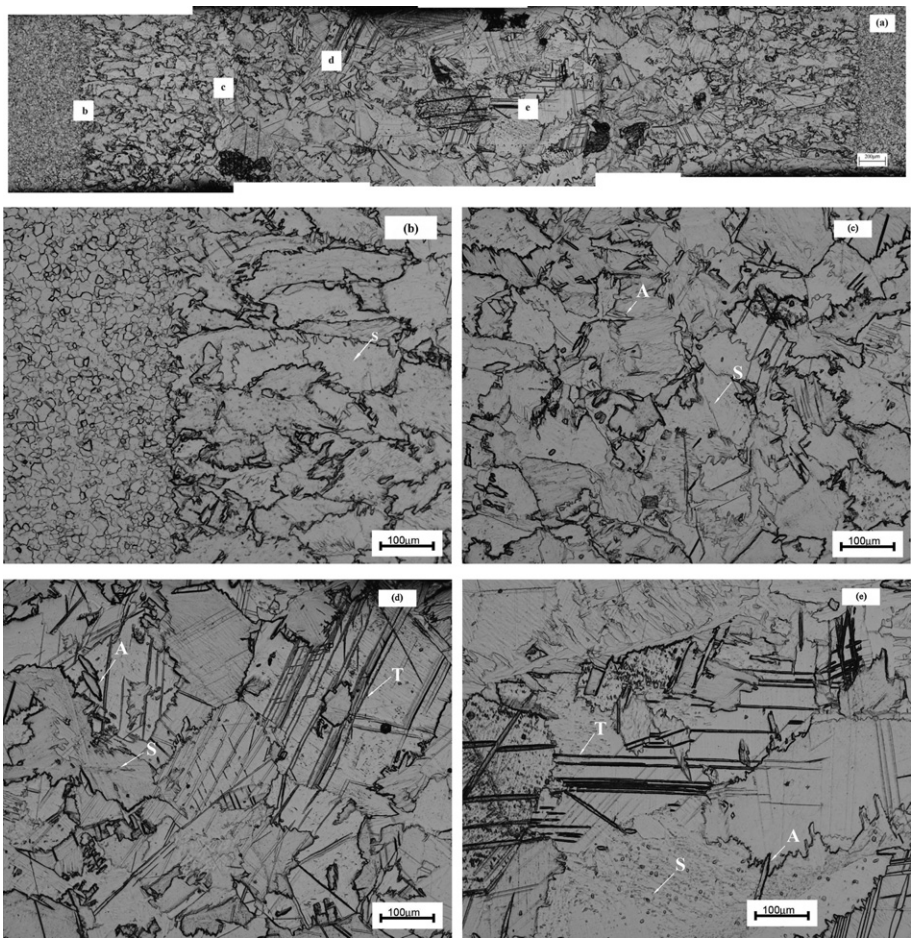

Fig. 8. Microstructures of laser-GMA hybrid welded joints at a laser power of 2 kW and a welding speed of 4 m/min: (a) low magnification micrograph showing the variation in microstructure across the weld; (b)–(e) higher magnification micrographs of regions marked sequentially from left to right in (a). Etchant: Kroll reagent.

orientation are found in the weld metal, especially near the weld centerline. The appearance of these twins reduces grain size of serrated alpha, and increases the amount of acicular. Although the hybrid welding process is deposited with a higher heat input than that used in the fiber laser welding process, it is obvious that the different alpha grains in the fusion zone of the hybrid welds have finer grain sizes than those of the fiber laser welds. This kind of microstructure made the good combination of strength and ductility in the butt joint of laser- GMA hybrid welding.

4. Conclusions

The following conclusions can be made from this work:

- A full-penetration weld with silver color was successfully obtained at welding speeds of up to 9 m/min in the laser-GMA hybrid and fiber laser welding process.
- Despite the difference in the microstructure of two kinds of welded joints, there was a remarkable similarity in the tensile strength and microhardness of the hybrid and laser welds. Both fiber laser and laser-GMAW hybrid welded joints showed higher microhardness and tensile strengths than the base metal. However, the hybrid welded joints had the good combination of strength and ductility.
- Only α-Ti phase have been identified for the fiber laser and hybrid welded joints. Coarse columnar alpha and a smaller amount of fine-grained acicular alpha appeared in the fiber laser welded joints. The microstructure in laser-GMA hybrid welded joint consisted of acicular alpha, platelet alpha and twins. This kind of microstructure made the good combination of strength and ductility in the laser-GMA hybrid welded joints.

Acknowledgements

The authors appreciate the support of the industrial partners in the Advanced Steel Processing and Products Research Center, Daido Steel Co., Ltd. at Japan.

References

[1] <http://www.ewi.org/uploads/insights/Spring2004_HeavyManufacturing.pdf>.
[2] Lee Won-Bae, Lee Chang-Young, Chang Woong-Seong, Yeon Yun-Mo, Jung Seung-Boo. Microstructural investigation of friction stir welded pure titanium. Mater Lett 2005;59:3315–8.
[3] Yunlian Qi, Ju Deng, Quan Hong, Liying Zeng. Electron beam welding, laser beam welding and gas tungsten arc welding of titanium sheet. Mater Sci Eng A 2000;280:177–81.
[4] Lathabai S, Jarvis BL, Barton KJ. Comparison of keyhole and conventional gas tungsten arc welds in commercially pure titanium. Mater Sci Eng A 2001;299:81–93.
[5] Uygur I, Dogan I. The effect of TIG welding on microstructure and mechanical properties of a butt-joined-unalloyed titanium. Metalurgija 2005;44(2):119–23.
[6] Danielson Paul, Wilson Rick, Alman David. Microstructure of titanium welds. Adv Mater Process 2003:39–42 [February].
[7] Denney Paul E, Shinn Brandon W, Mike Fallara P. Stabilization of pulsed GMAW in titanium welds with low-power lasers. In: Proceedings of 23rd international congress on applications of lasers and electro-optics (ICALEO); 2004. p. 10.

[8] <http://www.onr.navy.mil/sci_tech/3t/mantech/docs/news/NJC_WJ-MAY06.pdf>.
[9] Hiton Paul, Blackburn Jonathan, Chong Pak. Welding of Ti-6Al-4V with fiber delivered laser beams. In: Proceedings of 26th international congress on applications of lasers and electro-optics (ICALEO); 2007. p. 887–95.
[10] Liu J, Watanabe I, Yoshida K, Atsuta M. Joint strength of laser-welded titanium. Dental mater 2002;18:143–8.
[11] Schubert E, Wedel B, Kohler G. Influence of the process parameters on the welding results of laser-GMA welding. In: Proceedings of 21st international congress on applications of lasers and electro-optics (ICALEO); 2002. p. 10.
[12] Verwimp Jo, Gedopt Jan, Geerinckx Eric, Van Haver Wim, Dhooge Alfred, Criel Debby. Hybrid laser welding of dual phase steel DP600: microstructural and mechanical properties. In: Proceedings of 26th international congress on applications of lasers and electro-optics (ICALEO); 2007. p. 325–33.
[13] Eboo M, Steen WM, Clarck J. Arc augmented laser processing of materials. In: Proceedings of conference advances in welding processes. Harrogate, UK, 9–11(May); 1978. p. 257–65.
[14] Quintino L, Costa A, Miranda R, Yapp D, Kumar V, Kong CJ. Welding with high power fiber lasers – a preliminary study. Mater Design 2007;28:1231–7.
[15] Kancharla Vijay. Applications review: materials processing with fiber lasers under 1 kW. In: Proceedings of 25th international congress on applications of lasers and electro-optics (ICALEO); 2006. p. 579–85.
[16] Li X, Xie J, Zhou Y. Effects of oxygen contamination in the argon shielding gas in laser welding of commercially pure titanium thin sheet. J Mater Sci 2005;40:3437–43.
[17] Jaffee RI. Metallurgical synthesis. In: Jaffee RI, Burte HM, editors. Titanium science and technology, vol. 3. London: Pleunum Press; 1973. p. 1665–93.